# Spontaneous and cytokine-induced hole formation in epithelial cell layers: Implications for barrier function studies with the gingival cell culture, Gie-3B11, and other epithelial models

Elizabeth Rybakovsky[1], Nicole B. Buleza[2], Kevt'her Hoxha[2], Katherine M. DiGuilio[1], Elizabeth S. McCluskey[2], Cary L. Friday[1], Patrick J. Callaghan[1], Daniil V. Moskalenko[3], Biao Zuo[4], Sunil Thomas[1] and James M. Mullin[1,*]

[1]Lankenau Institute for Medical Research, 100 Lancaster Avenue, Wynnewood, PA 19096; [2]Department of Biology, Drexel University, Philadelphia, PA, 19104; [3]Department of Biology, Holy Family University, Philadelphia, PA, 19114; [4]Electron Microscopy Resource Laboratory, Department of Biochemistry & Biophysics, Perelman School of Medicine, University of Pennsylvania, Philadelphia, PA 19104, USA.

## ABSTRACT

Epithelial barrier function studies often attribute alterations in barrier function to induced changes in tight junctional (TJ) complexes. The occurrence of spontaneous and cytokine-induced, focal cell detachment in cell layers of the human gingival epithelial cell line, Gie-3B11, highlights the danger of this assumption without confirmatory experimentation. Gie-3B11 cell layers manifest morphological polarity, TJ complexes and barrier function after confluence but fail to then maintain a stable epithelial barrier. Transepithelial electrical resistance rises to over 100 ohms x cm$^2$ a few days after seeding cell layers at a confluent density, but then spontaneously declines, with simultaneous, inverse changes in transepithelial $^{14}$C-D-mannitol diffusion rates. This barrier decline correlates with the appearance of focal cell detachment/hole formation in cell layers. Both barrier compromise (decreased electrical resistance; increased $^{14}$C-D-mannitol leak) and hole formation are accelerated and exaggerated by exposing cell layers to proinflammatory cytokines. Both are inhibited by increasing the basal-lateral medium compartment volume, suggesting that cell layers are secreting factor(s) across their basal-lateral surfaces that are causal to hole formation. The molecular mechanism of cell death/detachment here is not as significant as the implications of hole formation for the correct interpretation of barrier function studies. Barrier changes in any epithelial model should be attributed to induced changes in TJ complexes only after thorough investigation.

## INTRODUCTION

In research on epithelial barrier function -and on epithelial tight junctions (TJs) -numerous epithelial cell culture models developed over the past several decades have greatly facilitated our growing understanding of the regulation of epithelial barriers in normal physiology and drug delivery, as well as in neoplasia, inflammation and infectious disease [1-7]. Differentiated epithelial cell culture models exist now for research in a wide variety of epithelial tissues: e.g. MDCK

*Corresponding author: MullinJ@mlhs.org

and LLC-PK$_1$ in renal tubular function [8, 9], CaCo-2, T$_{84}$ and HT-29/B6 for gastrointestinal epithelial studies [10-13], HEC-1A for uterine epithelial research [14-16], and so on. The cell culture models are imperfect due to phenotypic changes that occur during the transition from primary cell culture to established cell line [17], but the manifestation of cell polarity and the expression of an apically-situated, functional TJ complex between cells allows for the formation of a continuous cell layer in culture that can physically establish and functionally separate apical/luminal and basal-lateral/antiluminal fluid compartments - the hallmark characteristic of an epithelial tissue.

When a differentiated epithelial culture is trypsinized and its cells placed in suspension, cell polarity and TJ expression can be transiently lost, until the culture again achieves confluence, density-dependent inhibition and differentiation [18]. During this period, the cell layer may not manifest transepithelial electrical resistance (R$_t$) or the ability to impede the transepithelial diffusion of paracellular probe molecules such as fluorescein-labeled dextran, polyethyleneglycol, or D-mannitol. However, as the epithelial culture repolarizes and TJ proteins are expressed and organized, one can observe a steady rise in R$_t$, until a stable plateau level is achieved, as has been shown e.g. for CaCo-2 and T$_{84}$ cell layers [11, 19].

The gingival epithelial cell culture model, Gie-3B11, has retained in culture many differentiated features of its tissue of origin such as expression of the TJ protein, claudin-1, the cornified envelope protein, involucrin, the keratin-binding protein, filaggrin, and a gingival-like pattern of cytokeratin expression [20]. Most importantly, at confluence its cells can polarize and TJ complexes become synthesized, resulting in a functional epithelial barrier. As such, Gie-3B11 holds the promise of being a useful model for not only research on periodontal disease but for studying orally-acquired infections as well as oral neoplasia [21]. A human gingival epithelial cell line is particularly useful because the tissue of reference here, the gingival epithelium, cannot supply the amount of tissue for study that is available in e.g. gastrointestinal tissue. However, unlike the epithelial cell culture models mentioned

above, once Gie-3B11 establishes barrier function as manifested by R$_t$ values as high as 160 ohms x cm$^2$, it fails to maintain this barrier function, as evidenced by a decaying graph of R$_t$ as a function of time [20].

In this current study, we determine the cellular mechanism for this decrease of barrier function in Gie-3B11, and describe how this phenomenon - if unrecognized - can confuse the interpretation of many barrier function/TJ studies conducted using Gie-3B11. This recognition can be key in barrier function studies conducted with any epithelial cell culture model, not simply Gie-3B11. We also describe a method to suppress this loss of barrier function, as well as agents that accelerate barrier function decay.

## MATERIALS AND METHODS

### Cell culture

The Gie-3B11 cell culture, an immortalized human gingival keratinocyte cell line, was obtained from Applied Biological Material, Inc. (Richmond, BC, Canada), and was used between passages 2 and 16 (in our hands). When cells reached confluence, they were passaged by trypsinization (0.25% trypsin and 2.21 mM EDTA) (Mediatech, Inc., a Corning subsidiary, Manassas, VA) on a weekly basis. Cells were seeded at 2 x 10$^5$ cells per Falcon 75 cm$^2$ culture flask with 25 ml of Prigrow IV medium (Applied Biological Materials) supplemented with 2 mM L-Glutamine (Mediatech, Inc.) and 5% fetal bovine serum (Seradigm,VWR, Inc., Radnor,PA). Cultures were incubated at 37 °C in 95% air/5% CO$_2$ atmosphere.

### Treatment with cytokines

Human recombinant TNF-α, IL-1-β and IFN-γ were obtained from PeproTech, Inc. (Rocky Hill, NJ). Exposures of cytokines individually and in combination was as follows: 100 ng/mL TNF-α, 50 ng/ml IL-1-β and 200 ng/ml of IFN-γ were prepared in culture medium and applied to apical and basal-lateral sides of the cell layer for 48 h. Medium was filter sterilized with 0.2 μM disc filter units (Corning, Inc.). For antibody microarray analyses of pro-apoptotic factors produced by the Gie-3B11 cells, treatment with cytokines was only for 2.5 hours.

## Transepithelial electrophysiology and permeability

Cells were typically seeded into sterile Millicell polycarbonate (PCF) cell culture inserts (30 mm diameter with 0.4 μm pore size [EMD Millipore, Burlington,MA]), on day 0 at a seeding density of 5 x $10^5$ or 1 x $10^6$ cells/insert. Three to four Millicell PCF inserts were placed in either 100 mm petri dishes or 6-well dishes. On day 1, all cell layers were refed (2 ml apical/15 ml basal-lateral for inserts in 100 mm dishes; 2 ml apical/2 ml basal-lateral for inserts in 6-well dishes) with control medium containing 50 U/ml penicillin and 50 μgms/ml streptomycin. All cytokine treatments were begun 4 days post-seeding and exposure time of cytokines was 48 hours. Electrophysiological measurements and radiotracer flux studies with $^{14}$C-D-mannitol followed. On the day of transepithelial permeability experiments, the cell layers were refed with fresh control medium and allowed to incubate with fresh medium for 1.5-2 hours prior to electrophysiological readings. Transepithelial electrical resistance ($R_t$) was measured using 1 sec, 40 μamp direct current pulses, and calculated using Ohm's law. As soon as electrical measurements were completed, the basal-lateral medium was aspirated and replaced with 15 ml of radiolabeled medium containing 0.1 mM, 0.1 μCi/ml $^{14}$C-D- mannitol, $^{14}$C-polyethyleneglycol (4000 daltons) (Perkin-Elmer, Inc., Boston MA) or $^3$H-Lactulose (American Radiolabeled Chemicals, Inc., St. Louis, MO) and incubated at 37 °C for 90 minutes. Triplicate basal-lateral medium samples (50 μl) were then taken for liquid scintillation counting (LSC) for specific activity determination. Duplicate medium samples (250 μl) were taken from the apical fluid compartment for LSC to determine flux rates. The flux rate ($J_m$) in picomoles/min/cm$^2$ was calculated for $^{14}$C-D-mannitol and other radiolabeled paracellular probes diffusing across the cell layer using the specific activity determination.

## Hematoxylin stain

After completion of transepithelial resistance and mannitol flux studies, cell layers in Millicell PCF units were rinsed 5X with 0.154 M sodium chloride, then fixed with 50% methanol for 2 mins followed by 100% methanol for 2 mins. Hematoxylin stain (Thermo Fisher Scientific) was added for 5 mins and then cell layers were rinsed with tap water.

## Transmission electron microscopy

Tissues for electron microscopic examination were fixed with 2.5% glutaraldehyde, 2% paraformaldehyde in 0.1 M sodium cacodylate buffer, pH 7.4, overnight at 4 °C. After subsequent buffer washes, the samples were post-fixed in 2% osmium tetroxide for 1 hour at room temperature, and rinsed in deionized water prior to *en bloc* staining with 2% uranyl acetate. After dehydration through a graded ethanol series, the tissue was infiltrated and embedded in EMbed-812 (Electron Microscopy Sciences, Fort Washington, PA). Thin sections were stained with uranyl acetate and lead citrate and examined with a JEOL 1010 electron microscope fitted with a Hamamatsu digital camera and AMT Advantage image capture software.

## Cell lysates and antibody microarrays

Cell layers on Millicell PCF membranes were washed 5X in cold phosphate buffered saline following radiolabeled permeability studies. 600 ul of SDS-based lysis buffer with phosphatase and protease inhibitors [22] were added to each PCF unit and the cell layer was physically scraped off the polycarbonate membrane. The cell suspension was collected, flash-frozen at -80 °C and stored until processing for immunoblot analyses or microarrays. Lysate samples were submitted to Ray Biotech, Inc. (Norcross, GA) for the Human Apoptosis Array C1 analysis. Cytokine antibody array analyses were performed according to the manufacturer's instructions. Briefly, the array membranes were blocked for 30 min and then incubated with 1 ml of cell lysate sample described above. After washing the array membranes, 2 ml of diluted biotin-conjugated antibodies was added to the array membranes and the mixture was incubated on a shaker for 2 hr at RT. The array membranes were then washed again and incubated with horseradish peroxidase (HRP)-conjugated streptavidin for 2 hr at RT. After washing again, the signals were visualized using chemiluminescence detection system and quantified with UVP EpiChemi3 imaging system (Upland, CA). Signals from blank spots were used

as background. Final band intensities were calculated by subtracting the background from the original band intensities. Data were normalized to the positive controls and negative controls in the individual membranes.

### Culture medium antibody microarrays

On day 0, cells were seeded at a density of $5 \times 10^5$ per 4.2 cm$^2$ Millicell PCF insert in Prigrow media. Cells were refed in normal Prigrow medium on day 1 and day 4. On days 5 and 6, media samples were taken from the apical surface of the PCF and centrifuged to remove any cells. Three 500 ul supernatant samples were removed and stored at -80 °C. Three 500 ul control samples from the Prigrow media bottle were taken and stored at -80 °C. Samples were submitted to Ray Biotech, Inc. for the Human Cytokine Array 200 (Quantibody) performed as described above.

## RESULTS

### Morphological polarity and transepithelial physiology at confluence

Confluent Gie-3B11 cell layers manifest epithelial polarity and are capable of forming an intact epithelial barrier. Five days after seeding $5 \times 10^5$ or $1 \times 10^6$ cells into a 4.2 cm$^2$ Millicell PCF insert, cells manifested morphological polarity with a distinct apical microvillous membrane and with tight junctions (TJs) visible at the apical end of the intercellular space (Figure 1A).
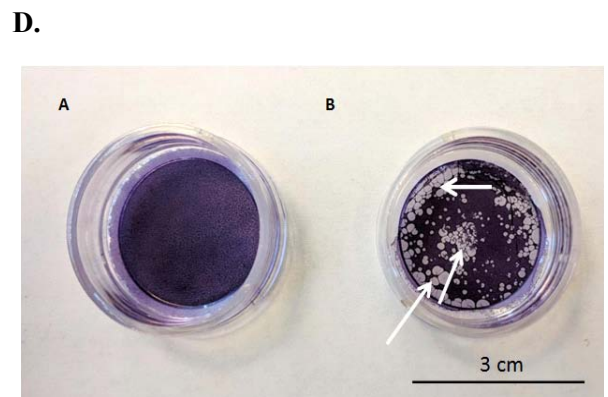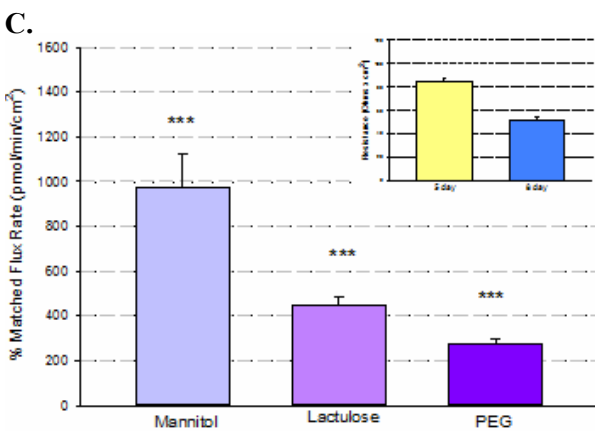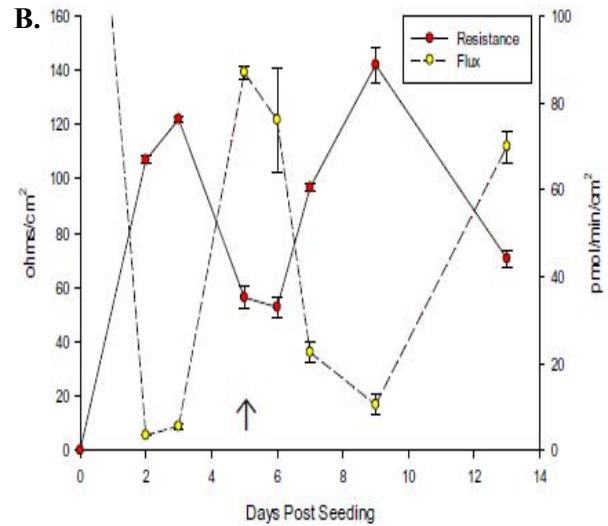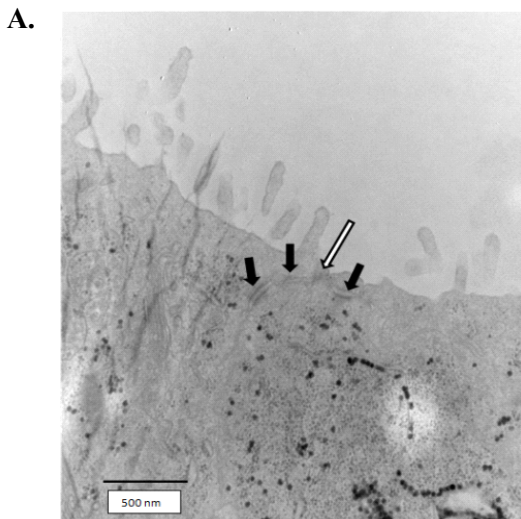


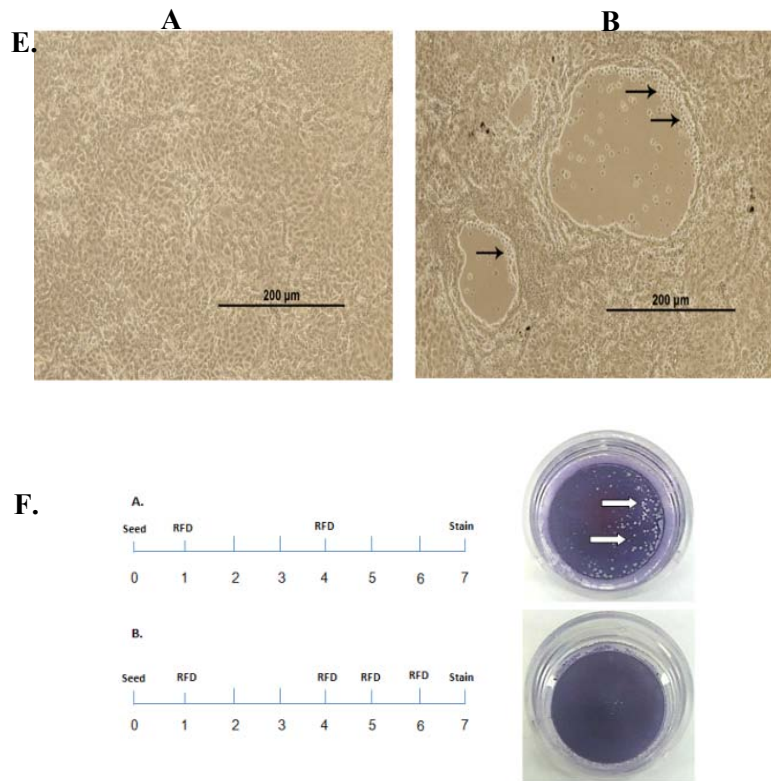**Figure 1**

Figure 1 continued..



**Figure 1. Panel A: Transmission electron micrograph of a post-confluent Gie-3B11 cell layer.** The cross section shown highlights the apical junctional region between two cells. Apical microvilli are abundant. Black arrows indicate desmosomal complexes. White arrow indicates a tight junctional complex. 57,000X. **Panel B: Effect of time post-seeding on transepithelial electrical resistance and transepithelial mannitol diffusion rate across Gie-3B11 cell layers.** Transepithelial electrical resistance ($R_t$) and transepithelial flux rate of $^{14}$C-D-Mannitol ($J_m$) were measured beginning 2 days post-seeding, as described in 'Materials and Methods' section; here seeding $1 \times 10^6$ cells per Millicell PCF on Day 0, and PCFs being placed in 6-well dishes instead of 100 mm petri dishes. Data are shown as mean ± standard error for n = 3 cell layers at each time point. The arrow indicates the point at which hole formation began to be observed by eye. **Panel C: Increase in transepithelial diffusion rates of three paracellular probes of increasing Stokes radius as hole formation occurs in Gie-3B11 barriers.** Data shown represent the mean ± standard error for n = 4 cell layers of the percentage increase in probe diffusion (leak) rate after hole formation (8-days-post-seeding) is observed, vs. pre-hole formation (5 days post-seeding). Flux rates were determined as described in 'Materials and Methods' section. ***indicates $P < 0.001$ (Student's t test, two-tailed) relative to the flux performed before hole formation was evident (5 days post-seeding). Inset shows the $R_t$ measurements performed on these cell layers before and after hole formation. **Panel D: Hematoxylin-stained Gie-3B11 cell layers in Millicell PCF inserts before and after hole formation.** Post-confluent cell layers were fixed and stained as described in 'Materials and Methods' section. Image A**:** Fully intact cell layer stained before hole formation is evident; Image B: Cell layer stained 8 days post-seeding with holes visible to the naked eye (white arrows). **Panel E: Phase contrast micrograph of Gie-3B11 post-confluent cell layer in active hole formation vs normal morphology.** Cell layer grown on glass coverslip as described in 'Materials and Methods' section, 48 hrs post-confluence. Regions without hole formation (**A**) and with hole formation (**B**) were photographed at 100X. Rounded cells which had not yet detached at the edges of holes are highlighted by black arrows. **Panel F: Culture medium refeeding suppresses hole formation in Millicell PCF units**. Cells were seeded into Millicell PCF units and refed the following day as described in 'Materials and Methods' section. The cell layers were then divided into two groups. Group A was refed every third day, followed by hematoxylin staining on day 7. Group B was refed on day 4 and then refed daily until staining on day 7. This experiment was repeated twice with similar results.

This differentiated morphology was consistent with results of standard physiological measurements of epithelial barrier function. Transepithelial electrical resistance ($R_t$) values as high as 80-130 ohms x cm$^2$ and concurrent mannitol permeability measurements ($J_m$) as low as 3-4 picomoles/min/cm$^2$ (for a 0.1 mM mannitol reservoir) were observed for this cell line [22]. This contrasts with $R_t$ values of typically 500-1000 ohms x cm$^2$ and $J_m$ values of 0.25 pmole/min/cm$^2$ for the stronger barrier function exhibited by CaCo-2 BBe cell layers [23] but a functional epithelial barrier was still evidenced nonetheless.

**Decline of barrier function in post-confluent cell layers: Hole formation**

However, whereas CaCo-2 and other widely used epithelial cell culture models maintain a characteristic $R_t$ value stably for days or even weeks after forming an epithelial barrier, Gie-3B11 cell layers spontaneously began to partially lose barrier function within only several days of first manifesting it (Figure 1B). In a time course of transepithelial electrical resistance ($R_t$) and transepithelial mannitol permeability ($J_m$), $R_t$ values increased as the epithelium formed (day 2 post-seeding), reaching almost 130 ohms x cm$^2$, but then spontaneously declined between days 3 and 5 (post seeding). $J_m$ values simultaneously, dramatically increased from approximately 5 pmoles/min/cm$^2$ to 95 pmoles/min/cm$^2$, as the $R_t$ values declined at day 5. Thereafter, both $R_t$ and $J_m$ values fluctuated (inversely to each other) out to day 13. Note that $J_m$ values never decreased to the level of the newly-formed epithelium on day 2. Transepithelial leakiness persisted out to and including day 13. Stable levels of $R_t$ and $J_m$ never form for this epithelial cell layer. The simultaneous increase of $J_m$ and decrease of $R_t$ suggested that this was not simply due to increased conductance of Na$^+$ and Cl$^-$ ions through tight junctions but rather a more generalized permeability increase. Note that the arrow in Figure 1B marks a time at which actual hole formation on the cell layer began to become evident (visible to the naked eye), as described below. Note also in Figure 1B that the decrease in $R_t$ and increase in $J_m$ did not simply continue but oscillated over the span of two weeks, suggesting that the compromise of epithelial barrier function

did not continue unabated once it began, but instead fluctuated with time, competing with barrier restitution by cell proliferation, migration and differentiation. In numerous studies of $R_t$ and $J_m$ as a function of days-post-seeding, we observed that the exact day(s) on which $R_t$ achieved its minimal value (and $J_m$ its maximal value) may vary from experiment to experiment, but the overall theme of impaired barrier function (decreased $R_t$ and elevated $J_m$) as days progressed, was consistent.

Using transepithelial paracellular probes of increasing molecular size (^{14}C-D-mannitol [180 daltons], ^{3}H-lactulose [360 daltons] and ^{14}C-polyethyleneglycol [4 kilodaltons]), we were able to observe that the increased barrier leakiness exhibited with time - and occurring during the decrease of $R_t$ - is extending to solutes at least as large as 4 kilodaltons, since increased transepithelial diffusion rates were observed for all three probes (Figure 1C). Here, cell layers at 5-days post-seeding were compared to cell layers 8 days post-seeding, when $R_t$ values were significantly lower. Mannitol leak increased by 970% in those cell layers manifesting lower $R_t$ values, while lactulose leak and polyethyleneglycol leak also increased, by 450% and by 270%, respectively. All increases were statistically significant. This suggests that at the time when $R_t$ is observed to be decreasing in these cell layers, the situation is not simply a change in permeability of TJs - unless the epithelial layer is suffering complete loss of TJ complexes - as is seen for example in calcium switch protocols [24]. Molecular sieving is clearly not evident in these now-leaky cell layers, since dramatically increased leak is seen for solutes at least as large as 4 kDa polyethyleneglycol. Although it is true that the magnitude of the increase in leak decreases as molecular probe size increases, this is not evidence for molecular sieving, but merely reflects the increased Stokes radius of the molecular probe, namely that larger molecules have lower rates of diffusion in free solution than smaller molecules.

The other possibility to explain the above $R_t$ and $J_m$ data, as well as the lactulose and polyethyleneglycol diffusion increase - as opposed to progressive increases in TJ permeability - is

complete loss of entire cells from the barrier, i.e. creation of actual holes. This would, of course, exhibit no size selectivity regarding transepithelial probe permeability. This in fact is what we observed to be occurring spontaneously in Gie-3B11 cell layers after the cell layer had fully formed. Within 24 hrs after $R_t$ values reached their maximum, a simple hematoxylin stain of cell layers in Millicell PCF inserts evidenced the appearance of circular holes in the epithelium, typically only 100-200 microns in diameter, invisible to the naked eye but readily visible in a dissecting microscope. We observed that these holes can then increase in size and number, and become easily visible to the naked eye (Figure 1D). This is accompanied by a continuous compromise of barrier function. Holes up to 8 mm in diameter were observed. Further increases in hole size can arise as holes coalesce in the cell layers. Typically we observed that the number and size of holes in these cell layers can oscillate with time over 14 days in culture, as reflected in oscillating values of $R_t$ and $J_m$ (Figure 1B). In fact we observed a close correlation between changes in $R_t$, changes in $J_m$, and frequency/size of holes.

This formation of actual holes in the cell layer begins with cell rounding and then complete detachment of cells, thereby increasing the diameter of the hole (see arrows in phase contrast micrographs in Figure 1E). Phase contrast microscope observations of cell layers on glass coverslips underscored that the phenomenon occurs in discrete foci that we see macroscopically as holes, rather than on a basis of (individual and random) single cell detachment/death throughout the cell layer. It is noteworthy that the phenomenon is very dependent on the substratum to which the cells are attached. We observed the appearance of holes in cell layers cultured on solid glass as well as on the polycarbonate membranes of Millicell PCF inserts. Appearance and enlargement of hole number and size in fact occurred most readily with cell layers grown on glass. We did not observe the phenomenon on tissue culture-treated plasticware (Falcon 75 cm$^2$ tissue culture flasks or Costar 6-well dishes), except occasionally along the very edges of a flask or dish. We also did not observe the phenomenon occurring in subconfluent cultures

on any substratum, as the phenomenon was restricted to post-confluent cultures. These properties of the phenomenon have likely contributed to hole-formation in Gie-3B11 cell layers being unrecognized and unreported in the published literature.

## Diminished hole formation as a result of increased culture medium refeedings

Although the findings presented herein might lead one to a conclusion that Gie-3B11 would never be suitable for studies of epithelial barrier function, this is not the case. We observed that a very frequent refeeding program of Gie-3B11 layers - daily after confluence is reached - can dramatically delay the appearance of holes, as well as reduce their frequency and size (Figure 1F). Cell layers that were maintained on a schedule of refeedings every 2-3 days developed hole formations earlier and with increased frequency and total area involvement. Those cell layers that were refed daily manifested delayed and reduced hole formation.

## Cytokine enhancement of hole formation and barrier compromise

Proinflammatory cytokines dramatically compromised the barrier function of Gie-3B11 cell layers. We observed that TNF-α treatment (1-100 ng/ml) significantly decreases $R_t$ and increases $J_m$ after a 48 hr exposure (Figure 2A). This is a commonly reported phenomenon in many different epithelial cell culture models [25, 26]. In epithelial cell culture models generally, it has been ascribed to both an induced leakiness in TJ complexes as well as induction of apoptosis on a random cell basis [27, 28]. The TNF-α -induced increase in $J_m$ also extended to increased leak of lactulose and polyethyleneglycol as well, underscoring the large scale leak that had developed. As shown in Figure 2B, although a very dramatic increase in $J_m$ was induced (over 800%) by TNF-α, statistically significant increases in lactulose leak (400%) and polyethyleneglycol (50% increase) were also occurring, similar to the leak profile exhibited with spontaneous hole formation (Figure 1C). TNF-α treatment of Gie-3B11 cell layers also increased the rate of appearance of hole formation, as well as the frequency and size of such holes. Whether hole formation
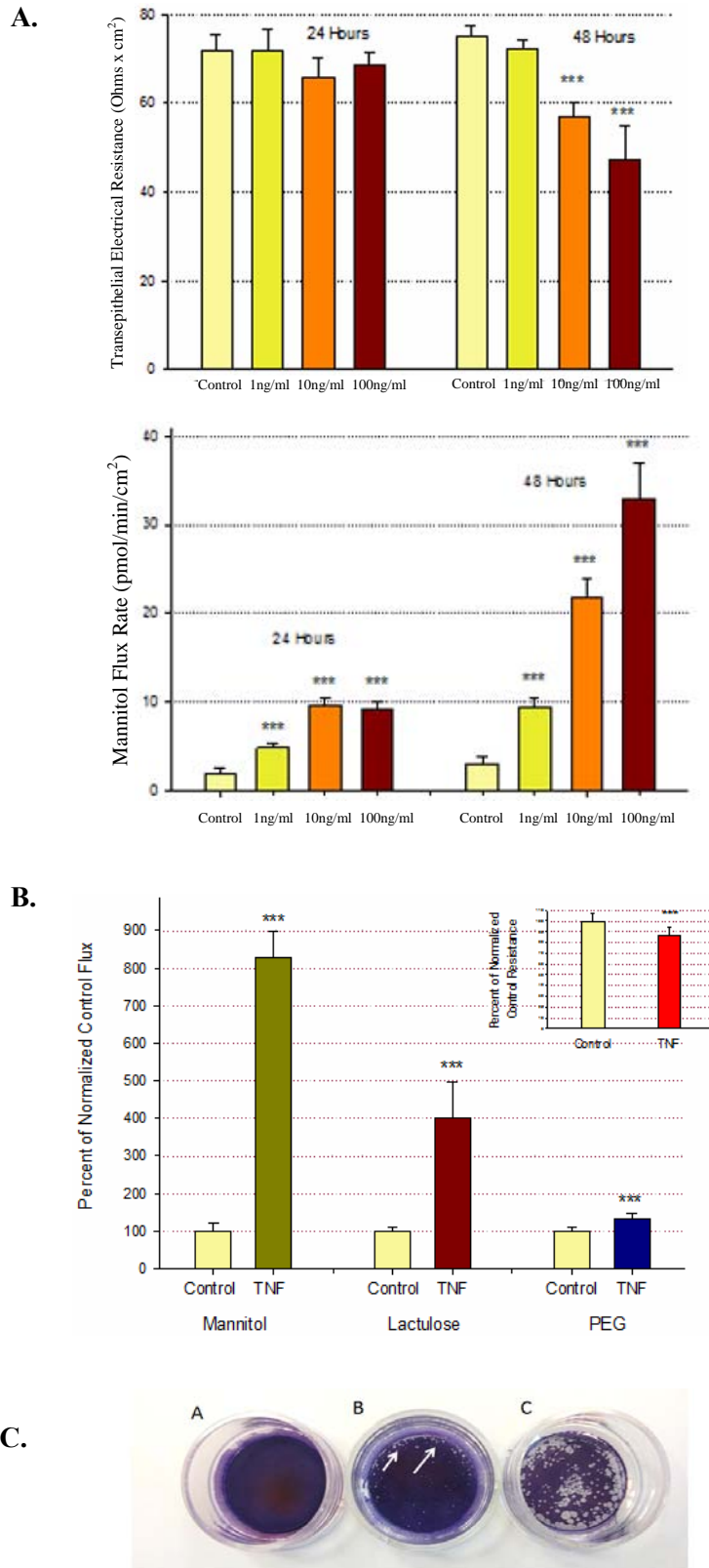
**A.**



**B.**



**C.**



**Figure 2**

was TNF-α-induced or spontaneous, we observed that hole formation often began along the outer edges of the cell layer (Figure 2C, image B). A combination of proinflammatory cytokines (TNF-α, IL1-β/IFN-γ) produced more extensive hole formation over the same time period than did TNF-α alone (Figure 2B, image C). The more extensive hole formation always correlated with exaggerated decreases in $R_t$ and increases in $J_m$. This occurred over time with spontaneous hole formation or hole formation following exposure to multiple cytokines as shown here. Hole formation would itself adequately explain the changes in $R_t$ and transepithelial leak of mannitol, lactulose and polyethyleneglycol, although a secondary effect on TJs cannot be ruled out.

## Lack of evidence of microbial pathogens

The peculiar circular patterns of the hole formation in these cell layers was not unlike the plaque formation that has been observed by many researchers in cell culture monolayers intentionally infected with certain viruses [29, 30]. This led us to test Gie-3B11 cell layers actively manifesting hole formation for the presence of pathogens common in human primary cell cultures (see Table S1 in Supplemental Material). The Gie-3B11 cultures were, however, negative for an array of common human viruses. Cultures were also continually screened for bacteria, fungi and mycoplasma (human and bovine), and tested negative as well. Cultures did test positive for the HPV16 viral protein, but this related back to the immortalization procedure by which the Gie-3B11 cell culture was established, not an actual HPV infection (note the negative result for HPV18).

One additional attempt to determine if the hole formation exhibited by Gie-3B11 was pathogen-based also proved negative. Culture medium was harvested from 5-day old Gie-3B11 cell layers manifesting active hole formation on glass coverslips. This conditioned culture medium was then added to subconfluent cultures of CACO-2 human gastrointestinal epithelia and 293T human kidney cells. These cell cultures were left exposed to this culture medium for 18-20 hrs before it was removed and cultures were refed with normal medium. After later achieving confluence, these cultures were trypsinized and replated on glass coverslips and observed for formation of holes post confluence. Results were consistently negative as hole formation in these new cultures was never observed.

## Protein microarray analyses of culture medium and cell lysates from hole-forming cell layers

Again using Gie-3B11 cultures actively manifesting hole formation, we performed defined protein microarrays on both cell lysates as well as conditioned culture medium. In studies involving protein microarrays on conditioned medium taken from the apical fluid compartment of cell layers exhibiting active hole formation, we observed significant and dramatic increases in the proinflammatory cytokine proteins, LIF, MIF and

**Figure 2. Panel A: Effect of TNF-α on transepithelial electrical resistance ($R_t$) and transepithelial $^{14}$C-D-mannitol diffusion rate ($J_m$).** Cell layers in Millicell PCF inserts were treated with TNF-α at varying concentrations for 24 and 48 hrs followed by measurements of $R_t$ (upper bar graph) and $J_m$ (lower bar graph) as described in 'Materials and Methods' section. Data shown represent the mean ± standard error for n = 4 cell layers. ***indicates P < 0.001 (Student's t test, one-sided). **Panel B: Effect of TNF-α on transepithelial diffusion rates of D-mannitol, lactulose and polyethyleneglycol across control vs TNF-α-treated cell layers.** Transepithelial flux studies were performed as described in 'Materials and Methods' section across control vs TNF-α-treated (100 ng/ml, 48 hrs) cell layers (5-days-post-seeding) for $^{14}$C-D-mannitol, $^{3}$H-lactulose and $^{14}$C-polyethyleneglycol. Data shown represent the mean ± standard error for n = 8 cell layers. ***indicates P < 0.001 (Student's t test, one-sided). Inset shows the $R_t$ measurements performed before the diffusion rate studies on control and TNF-α-treated cell layers. **Panel C: Hematoxylin-stained Gie-3B11 cell layers in Millicell PCF inserts showing increased hole formation in cytokine-treated cell layers.** Cell layers were treated with TNF-α (100 ng/ml) or TNF-α (100 ng/ml) + IL1-β (50 ng/ml) + IFN-γ (200 ng/ml) for 48 hrs followed by hematoxylin staining as described in 'Materials and Methods' section. A 5-day-post-seeding confluent control cell layer in a Millicell PCF insert showing no hole formation **(A)** is compared to a 7-day-post-seeding TNF-treated cell layer showing numerous holes along its outer area **(B)**. A 7-day-post-seeding TNF/IL1-β/IFN-γ-treated cell layer **(C)** exhibits more extensive hole formation, with holes spreading into the more central region of the cell layer.

Tarc, and the anti-apoptotic proteins, OPN, TRAIL-R4 and VEGF-C (see Figure S1 in Supplemental Material). In a separate study, we analyzed cell layers treated for 2.5 hrs with TNF-α alone and with a combination of TNF-α (100 ng/ml), IL1-β (50 ng/ml) and interferon-γ (200 ng/ml). Both conditions induced substantial leak and hole formation in the Gie-3B11 cell layers. In studies performed on duplicate cell layers for each condition, we noticed no dramatic change of any apoptotic or cell cycle regulatory protein tested (PARP, elF2α, Erk1/2, hsp27, ikBα, JNK, NFkB, p38, p53, SMAD2, TAK1) except for the cell cycle inhibitor, p27, which decreased by 25% in the presence of TNF-α, and by 35% (P < 0.05) in the presence of TNF-α/IL1-β and IFN-γ (Figure S2, Supplemental Material). Interpretation of these and other molecular findings bearing upon hole formation in the cell layer should take into account that hole formation is occurring in tandem with increased proliferation/motility of surviving cells as the cell layer attempts to "fill in" the sites of damage/detachment.

## DISCUSSION

This paper serves to: 1) describe a unique perturbation of epithelial barrier function in a gingival epithelial cell culture model; and 2) issue a general caveat about the need for careful interpretation of the cellular nature of induced changes in epithelial barrier function in any epithelial or endothelial cell culture model.

We describe in this study a process of spontaneous hole formation in differentiating cell layers of the Gie-3B11, human gingival epithelial cell line. We explore its ramifications for barrier function studies conducted with this - and other - epithelial models. Other than demonstrating acceleration of the process by proinflammatory cytokines, and its retardation by frequent changes of culture medium, we provide only very limited contributions concerning potential molecular mechanisms underlying the process. As one fundamental example, we cannot as yet even state whether hole formation is due to cell detachment followed by cell death, or, in fact, the reverse. Similarly, we cannot state whether the process of cell death here proceeds *via* apoptosis, necrosis

or autophagy. The consistent acceleration of the process by proinflammatory cytokines (Figure 2) seems to argue for apoptotic cell death being involved, but the increase of the anti-apoptotic proteins, OPN, TRAIL-R4 and VEGF-C, in cell layers actively forming holes (see Supplemental Material), suggests otherwise. Clearly more work is needed to determine what underlies and drives the phenomenon, but an appreciation of the existence of the phenomenon and its implications (the cellular mechanism) is essential to correct interpretation of barrier function studies undertaken with this cell culture, and possibly others as well.

In continuous studies stretching over 18 months, we have observed that this phenomenon of Gie-3B11 hole formation is also quite variable. The dependence of the phenomenon on cell seeding density and refeeding schedule both contribute to this variability. Hole formation also depends upon the volume of the basal-lateral medium compartment (hole formation being greater in PCFs in 6-well dishes [2 ml basal-lateral compartment per PCF] compared to hole formation in PCFs in 100 mm petri dishes [5 ml basal-lateral compartment/PCF]) (data not shown). Increased frequency of refeeding also reduced the magnitude of hole formation (Figure 1F).

We also observed that the substratum on which cell layers adhere additionally contributed to the presence and intensity of the phenomenon. For example, we never observed the spontaneous formation of holes in Gie-3B11 cell layers grown in culture flasks (Falcon 75 cm² [Corning, Inc.]) whereas the phenomenon always occurred consistently and spontaneously in cell layers attached to glass coverslips. The phenomenon was never seen in subconfluent cultures on any substratum. Similarly, although we consistently observed that hole formation occurred on the polycarbonate membrane supports of the Millicell PCF cell culture insert, we never observed hole formation on Anocell (Whatman, Inc) cell culture inserts. The hole formation that occurred in Transwell cell culture inserts (Corning, Inc.) was markedly less than we observed in Millicell PCFs. In fact, we observed differences in the intensity of hole formation on Millicell PCF cell culture

inserts depending on the lot number of the inserts (data not shown).

An investigator whose focus is on epithelial TJ regulation, and is interested in the effect of a protein or small molecule drug on the barrier function of an epithelial cell culture model, often has a certain bias as to the interpretation of any induced decrease in $R_t$ values or elevation of $J_m$ values, relating back to their initial hypothesis. That bias could easily lead to an interpretation that, for example, an observed decrease in $R_t$ was due to the applied small molecule drug or protein altering TJs and increasing their permeability. An observed decrease in $R_t$ or increase in $J_m$ could just as easily be due however to a cytotoxic effect of the drug or protein under study, resulting in cell death and detachment, and resultant holes in the cell layer. Decreased $R_t$, for example, signifies increased conductance of $Na^+$ and $Cl^-$ ions across the cell layer. It is an average reading reflecting paracellular conductance across a broad area of the cell layer. That increased conductance could be through defined areas denuded of cells ("holes") or it could be increased ion flow through altered TJs. A decreased $R_t$ does not - by itself - distinguish which outcome.

In Figure 1B, one can observe that there is a much greater percentage change in $J_m$ than there is in $R_t$. Unlike $J_m$, which would increase in simple proportion to the increase in total hole surface area across the cell layer, $R_t$ - the inverse of conductance - constitutes a more complex parameter. First, consider that there is significant transepithelial $Na^+$ permeability across even control TJs. This results in there being - even initially - two significant paracellular diffusion pathways which exist in parallel: 1) limited but significant permeation across an extremely large number of junctional pairings; and 2) virtually unrestricted permeation across a limited area constituted by the holes that have formed. The rules of parallel resistances then apply $(1/R_t = 1/R_1 + 1/R_2)$. Second, one must consider that unlike $J_m$, $R_t$ is an inverse relationship. Taken together, changes in $R_t$ will thus of necessity be numerically less than those in $J_m$, and this is evident in Figure 1B.

These two very different cellular-level mechanisms - induced TJ leak or hole formation - were jointly examined over 20 years ago in studies on the effect of the cytokine, TNF-α, on the barrier function of the LLC-PK$_1$ renal epithelial cell layer [28, 31]. Here it was concluded that TNF-α was decreasing barrier function in part by inducing apoptosis in the cell layer - but not actual hole formation. Immunofluorescence microscopy showed that TNF-α-induced cell death was not leading to cell detachment and holes. Instead, phagocytosis of single, individual apoptotic cells by healthy adjacent epithelial cells allowed for removal of these apoptotic cells by a processing mechanism that prevented actual hole formation. It was a conclusion requiring extensive histological and ultrastructural studies.

Gitter et al. [27] used TNF-α to increase the number of apoptotic cells in an HT-29/B6 epithelial cell layer, and then used the conductance scanning technique to show that TNF-α was both inducing leak in TJs throughout the epithelial layer as well as inducing leak at a finite number of apoptotic cells in the cell layer. Using a combination of conductance scanning and immunofluorescence microscopy, their work showed that the sites of apoptotic cells were partially leaky (with respect to the non-apoptotic areas of the cell layer) but, as was also true for the LLC-PK$_1$ cell layers, there were not actual holes. TNF-α treatment of LLC-PK$_1$ cell layers caused a small and barely significant increase in transepithelial diffusion of PEG, but with no increase in radiolabeled dextran flux of 10 kDa and 70 kDa species - additional evidence of the lack of actual hole formation here [32]. Bojarski et al. [33] induced apoptosis in HT-29/B6 intestinal epithelial cell layers with camptothecin, and interestingly observed that whereas mannitol and lactulose flux increased, flux of 4 kDa polyethyleneglycol did not. This finding was likewise again in keeping with the fact that the apoptotic cells being induced did not detach from the cell layer and leave actual holes in the cell layer. These previous studies contrast strongly with our current finding for Gie-3B11

cell layers treated with TNF-α - where in addition to increased leak to mannitol and lactulose, polyethyleneglycol leak also increased significantly (Figure 2B).

Conductance scanning and immunofluorescence microscopy could certainly reveal the presence of actual holes in an epithelium - the situation we find both spontaneously arising in Gie-3B11 cell layers, as well as being induced by TNF-α. However, most laboratories engaged in transepithelial barrier function studies are not equipped to perform conductance scanning. Moreover, most such laboratories would also not have a reason to stain their cell layers conventionally or use immunofluorescence techniques and thereby detect hole formation in that manner. These laboratories will typically only measure resistance or impedance across the entire cell layer as an average value, using commercially available instrumentation such as EVOM. Nor will mannitol or fluorescein permeability measurements detect hole formation either (as opposed to induced TJ leak), because these permeability studies are also average measurements across an entire cell layer. Such laboratories could thus easily conclude that TJ leak had increased as a result of some agent or treatment, whereas in fact, hole formation was the reason for decreased $R_t$ and increased $J_m$. At a time when the majority of published barrier function studies are coming from research groups in immunology or cancer biology or infectious disease or nutrition (as opposed to epithelial cell biology/cell physiology research groups), this is a particularly valid concern.

The fact that hole formation in Gie-3B11 cell layers will occur spontaneously - and not require TNF-α - creates an even more challenging situation for barrier function studies conducted with this model. However, we have shown that a daily schedule of culture medium refeeding will forestall hole formation (Figure 1F). One can therefore effectively use Gie-3B11 in barrier function studies, but one must monitor for the presence of hole formation as well as take active measures to prevent it. The spontaneous nature of hole formation here may in fact be linked to Gie-3B11 cells secreting proinflammatory cytokines (Figure S1, Supplemental Material). These cells' tendency to also synthesize and secrete known *anti*-apoptotic proteins creates questions as to the exact nature of the cell death that is occurring here, which will be a subject of future research by our group. Inhibition of the phenomenon of hole formation by refeeding suggests that culture medium pH and cellular metabolic activity should also be investigated as contributors to the phenomenon. For now we can merely point out that this phenomenon can be spontaneous, but also be accelerated by exposure to cytokines. Exposure to a combination of TNF-α, interleukin-1-β and interferon-γ, accelerates this process even more than that which occurs with TNF-α exposure alone (Figure 2C).

We term this process of hole formation in these cell layers, *opiplasi* (from the Greek, *opi* = hole and *plasi* = formation/creation). Although the phenomenon obviously complicates study of epithelial barrier function, the phenomenon could have wide application in cancer research by way of targeted induction of cell death in transformed/ neoplastic cell populations *in vivo*. It is worth noting that the hole formation that is observed here- and the cell death/detachment that underlies it- seems to reach an uneven and changing balance where the rate of cell restitution can match, equal or exceed the rate of cell death, causing dramatic and oscillating changes in barrier function (see Figure 1B).

In this study we described the process of spontaneous hole formation in cell layers of the gingival epithelial model, Gie-3B11, and its impact on interpretation of barrier function studies involving this model. We also however suggest that this is a larger issue encompassing other epithelial cell culture models as well. We have highlighted this issue with regard to cytokine treatment of the LLC-PK$_1$ renal cell culture model and the HT-29/B6 intestinal cell culture model. The phenomenon of spontaneous hole formation must be considered for any new epithelial cell culture model that one may study, as Gie-3B11 is not unique in this respect, since LLC-PK$_1$ cell layers have also spontaneously exhibited such behavior [34].

## CONCLUSION

In summary, we demonstrate here that a new epithelial barrier model, the human gingival epithelial cell line, Gie-3B11 -with application to both periodontal research and orally-acquired infections and neoplasia- exhibits a unique (and to date, overlooked) phenomenon that can dramatically affect the interpretation of studies conducted on it. This is the spontaneous -as well as cytokine-induced- formation of millimeter-sized holes in the epithelial barrier that can obscure or confuse any effects on the permeability of the cell layer's TJs. Our current study highlights a very important finding for investigators using the Gie-3B11 model, but it also should urge caution for researchers using any epithelial cell culture model -that compromised epithelial barrier function should not simply be ascribed to increased leakiness of TJs, but could instead arise due to a variety -and in fact a combination- of effects on the barrier.

## ACKNOWLEDGEMENTS

## AUTHORS' CONTRIBUTION

Elizabeth Rybakovsky: involved in all experiments in this study; maintained laboratory notebook on studies; assisted in data analysis; critical reading of manuscript; preparation of all written methods' descriptions.

Nicole Buleza, Patrick Callaghan, Daniel Moskalenko, Cary Friday, Katherine DiGuilio, Elizabeth McCluskey: performed cell culturing and select physiology experiments; assisted in data analysis.

Kevther Hoxha, Patrick Callaghan and Daniel Moskalenko: performed staining of cell layers and quantitative assessments of hole formation.

Sunil Thomas: assisted in protein microarray studies; critical reading of manuscript.

Biao Zuo: preparation of specimens for and performance of transmission electron microscopy.

James M. Mullin: planning of study and individual experiments; data analysis; preparation of manuscript.

## CONFLICT OF INTEREST STATEMENT

There is no perceived or potential conflict of interest, financial or otherwise.

## SUPPLEMENTAL MATERIAL

**Table S1. Antibody-based pathogen testing on Gie-3B11 cell layers exhibiting active hole formation.** Gie-3B11 cell layers were analyzed by Idexx, Inc. (h-IMPACT Virus Panel) for the presence of specific pathogens. Cells were seeded onto glass coverslips. Hole formation was observed 2 days post confluence at which time cell layers were scraped and frozen at -80 °C for subsequent testing. **HPV16 was used as the immortalizing agent for the GIE-3B11 cell line (Groeger *et al*., 2008), hence the positive result in this panel. *Mycoplasma tests were routinely performed on the Gie-3B11 cell cultures used here and have been consistently negative over two years. "+" = positive; "-" = negative.

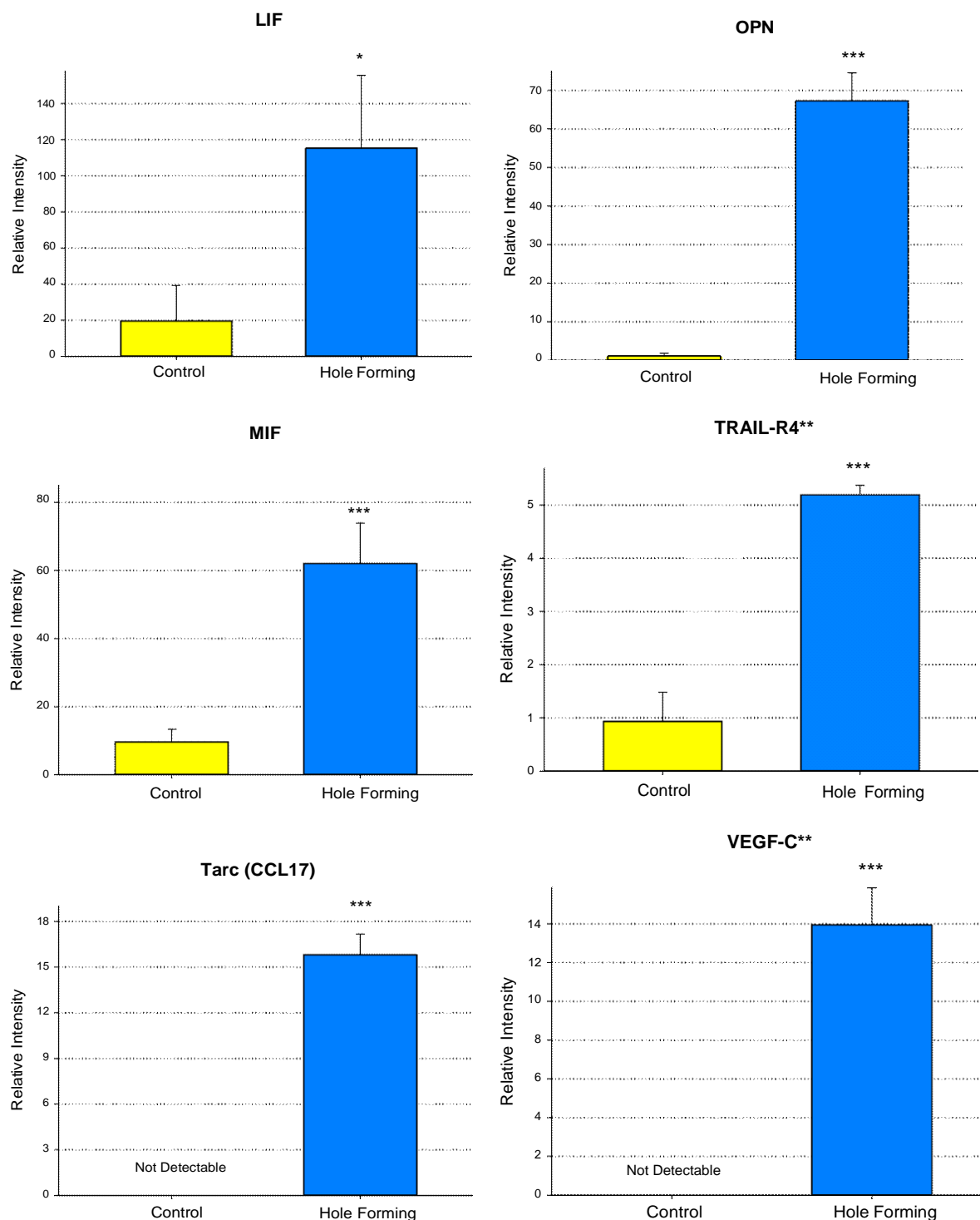| Pathogens Screened | Results |
|---|---|
| EBV | – |
| HAdV | – |
| HCMV | – |
| Hepatitis A | – |
| Hepatitis B | – |
| Hepatitis C | – |
| HHV 6 | – |
| HHV 8 | – |
| HIV1 | – |
| HIV2 | – |
| HPV16 | +** |
| HPV18 | – |
| HSV 1 | – |
| HSV 2 | – |
| HTLV 1 | – |
| HTLV 2 | – |
| VZV | – |
| Hantaan | – |
| LCMV | – |
| *Mycoplasma sp.* | – |
| Seoul | – |
| Sin Nombre | – |
| *Treponema pallidum* | – |

**Figure S1. Increase in proinflammatory and anti-apoptotic protein synthesis and secretion during hole formation.** Cell layers seeded on day zero were refed on day 1 and day 4. Apical culture medium was sampled on days 5 and 6. Hole formation was not visible on day 5, but was obvious on day 6. Protein (antibody) microarrays were performed by Ray Biotech, Inc. as described in 'Materials and Methods' section. Data shown represent signal intensity for the protein indicated in apical medium from 3 cell layers $\pm$ standard error, on the two time points. *indicates $P < 0.05$; ***indicates $P < 0.001$ (Student's t test, two-tailed).
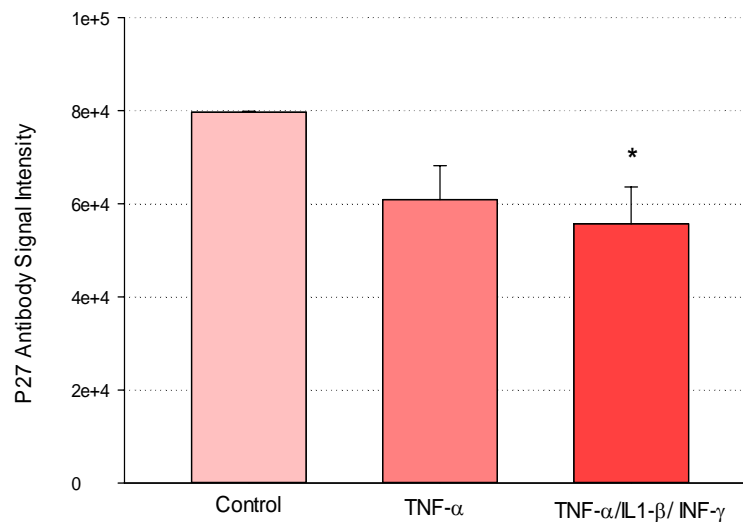
**Figure S2. Decrease of the cell cycle inhibitory protein, p27, in cell layers treated with pro-inflammatory cytokines.** On day 4 post-seeding, cell layers were refed with fresh medium $\pm$ TNF-$\alpha$ (100 ng/ml), IL1-$\beta$ (50 ng/ml) and interferon-$\gamma$ (200 ng/ml). Protein (antibody) microarrays were performed on cell lysates by Ray Biotech, Inc. as described in 'Materials and Methods' section. Results shown represent antibody signal intensity for duplicate cell layers refed with control medium, TNF-$\alpha$ medium, and TNF-$\alpha$/ IL1-$\beta$/IFN-$\gamma$ medium, after 2.5 hrs. *indicates $P < 0.05$ (Student's t test, two-tailed).

## REFERENCES

1. Abbott, N. J. 2005, Cell Mol. Neurobiol., 25, 5-23.
2. Bhowmick, R. and Gappa-Fahlenkamp, H. 2016, Lung, 194, 419-428.
3. Guttman, J. A. and Finlay, B. B. 2009, Biochim. Biophys. Acta., 1788, 832-841.
4. McCaffrey, L. M. and Macara, I. G. 2011, Trends Cell Biol., 21, 727-735.
5. Pereira, J. F., Awatade, N. T., Loureiro, C. A., Matos, P., Amaral, M. D. and Jordan, P. 2007, Cell Mol. Life Sci., 73, 3971-3989.
6. Rizzolo, L. J. 2014, Exp. Eye Res., 126, 16-26.
7. Sousa, S., Lecuit, M., and Cossart, P. 2005, Curr. Opin. Cell Biol., 17, 489-498.
8. Mullin, J. M., Weibel, J., Diamond, L. and Kleinzeller, A. 1980, Journal of Cellular Physiology, 104, 375-389.
9. Rindler, M. J., Chuman, L. M., Shaffer, L., and Saier, M. H. Jr., 1979, J. Cell Biol., 81, 635-648.
10. Bode, H., Schmidt, W., Schulzke, J. D., Fromm, M., Riecken, E. O. and Ullrich, R. 2000, Ann. NY Acad. Sci., 915, 117-122.
11. Hidalgo, I. J., Raub, T. J. and Borchardt, R. T. 1989, Gastroenterology, 96, 736-749.
12. Kreusel, K. M, Fromm, M, Schulzke, J. D., and Hegel, U. 1991, Am. J. Physiol., 261, C574-582.
13. Madara, J. L, Stafford, J., Dharmsathaphorn, K. and Carlson, S. 1987, Gastroenterology, 92, 1133-1145.
14. Castagnetta, L, Granata, O. M., Lo Casto, M., Miserendino, V., Calo, M. and Carruba, G. 1986, J. Steroid Biochem., 25, 803-809.
15. Kuramoto, H, Tamura, S. and Notake, Y. 1972, Am. J. Obstet. Gynecol. 114, 1012-1019.
16. Wild, M. J., Rudland, P. S. and Back, D. J. 1993, J. Steroid Biochem. Mol. Biol., 45, 407-420.
17. Becker, J. H. and Willis, J. S. 1979, J. Cell Physiol., 99, 427-439.
18. Griepp, E. B., Dolan, W. J., Robbins, E. S. and Sabatini, D. D. 1983, J. Cell Biol. 96, 693-702.
19. Madara, J. L. and Dharmsathaphorn, K. 1985, J. Cell Biol., 101, 2124-2133.
20. Groeger, S., Michel, J. and Meyle, J. 2008, J. Periodontal Res., 43, 604-614.
21. Groeger, S., Jarzina, F., Windhorst, A. and Meyle, J. 2016, J. Periodontal Res., 51, 748-757.

22. Rybakovsky, E., Valenzano, M. C., Deis, R., DiGuilio, K. M., Thomas, S. and Mullin, J. M. 2017, J. Agric. Food Chem., 65, 10950-10958.

23. Valenzano, M. C., DiGuilio, K., Mercado, J., Teter, M., To, J., Ferraro, B., Mixson, B., Manley, I., Baker, V., Moore, B. A., Wertheimer, J. and Mullin, J. M. 2015, PLoS One, 10, e0133926.

24. Stuart, R. O., Sun, A., Panichas, M., Hebert, S. C., Brenner, B. M. and Nigam, S. K. 1994, J. Cell Physiol., 159, 423-433.

25. Ma, T. Y., Iwamoto, G. K., Hoa, N. T., Akotia, V., Pedram, A., Boivin, M. A. and Said, H. M. 2004, Am. J. Physiol. Gastrointest. Liver Physiol., 286, G367-376.

26. Mullin, J. M. and Snock, K. V. 1990, Cancer Res., 50, 2172-2176.

27. Gitter, A. H, Bendfeldt, K., Schulzke, J. D. and Fromm, M. 2000, FASEB J., 14, 1749-1753.

28. Peralta Soler, A., Mullin, J. M., Knudsen, K. A. and Marano, C. W. 1996, Am. J. Physiol. 270, F869-79.

29. Shimonaski, G. and Came, P. E. 1970, Appl. Microbiol., 20, 775-777.

30. Consigli, R. A., Zabielski, J. and Weil, R. 1973, Appl. Microbiol., 26, 627-628.

31. Soler, A. P., Miller, R. D., Laughlin, K. V., Carp, N. Z., Klurfeld, D. M., Mullin, J. M. 1999, Carcinogenesis, 20, 1425-1431.

32. Mullin, J. M., Marano, C. W., Laughlin, K. V., Nuciglio, M., Stevenson, B. R. and Soler, P. 1997, J. Cell Physiol., 171, 226-233.

33. Bojarski, C., Gitter, A. H., Bendfeldt, K., Mankertz, J., Schmitz, H., Wagner, S., Fromm, M. and Schulzke, J. D. 2001, J. Physiol., 535, 541-552.

34. Mullin, J. M., Weibel, J., Diamond, L. and Kleinzeller, A. 1981, Proceedings of the 28th International Congress of Physiological Sciences, Budapest, Hungary, L. Takacs (Ed.), Pergamon Press, Oxford, UK, 175-179.